Journal of Engineering Science and Technology
Vol. 16, No. 2 (2021) 1196 - 1212

OPTIMIZATION OF ECONOMIC ENVIRONMENTAL AND SOCIAL BENEFITS FOR INTEGRATED ENERGY SYSTEMS

DUY C. HUYNH[1,*], LOC D. HO[1], MATTHEW W. DUNNIGAN[2]

[1]School of Engineering, Ho Chi Minh City University of Technology (HUTECH), Ho Chi Minh City, Vietnam
[2]School of Engineering and Physical Sciences, Heriot-Watt University, Edinburgh, United Kingdom
*Corresponding Author: hc.duy@hutech.edu.vn

Abstract

An optimal operating strategy is proposed for integrated energy systems under economic, environmental, and social benefits based on a modified cuckoo search (MCS) algorithm. Each optimal operating strategy is a solution to a multi-objective optimization problem with non-linear constraints. The MCS algorithm is applied for finding out the optimal operating strategy of integrated energy systems. The cuckoo search (CS) algorithm is modified to increase the convergence speed where the first modification relates to the size of the Lévy flight step size and the second modification includes the addition of information exchange between the top eggs or the best results. The proposal is implemented to the integrated IEEE 10-generator energy system. The obtained results confirm the proposal's effectiveness for optimization of economic, environmental, and social benefits of integrated energy systems. The particle swarm optimization (PSO) and CS algorithms are used to make comparisons showing the superiority of the MCS algorithm, as well as confirming the MCS algorithm's potential, especially in integrated energy systems.

Keywords: Cuckoo search algorithm, Integrated energy systems, Optimization.

1. Introduction

The classical optimal operating problem is to search an optimal operating strategy for generators [1-9]. Furthermore, due to environmental concerns arising from the emissions produced by fossil-fuelled thermal power plants, the classical problem of optimization can no longer be only considered to optimize the total cost of fuel. The environmental problem is proposed to optimize the emissions of sulphur oxides, SO_x and nitrogen oxides, NO_x caused by fossil-fuelled thermal power plants [10-13].

Additionally, it is important that the generated power has to be provided reliably to society. There is also a social impact on power outages [14]. This paper presents the optimal operating problem, taking into account the economic, environmental, and social benefits. Especially, the problem is applied for an integrated energy system including thermal, wind and solar power plants [8, 14-22]. Obviously, the integrated energy system depends on uncontrollable natural conditions creating difficulties in the optimization.

There has been much research using various approaches to solve the optimal operating problem such as a distributed algorithm of the convex relaxation and dual decomposition which does not require any initialization process and robust to various changes [1]; an application of barnacles mating optimizer which is based on the behaviour of barnacles seeking of mating [2]; a combination of a bee algorithm and tabu search algorithm [3]; a particle swarm optimization algorithm [4, 8]; a teaching learning based optimization technique which is inspired by the teaching and learning process in a classroom environment [5]; a stochastic whale optimization algorithm [6]; an adaptive piecewise-quadratic under-approximation [7]; a cuckoo search algorithm [9, 11]; an evolutionary algorithm [10, 13, 15], etc.

It can be realized that there has recently been a significant number of modern meta-heuristic algorithms proposed for solving the optimal operating problem. These algorithms which are emerging and becoming increasingly popular are inspired by nature. There are two main characteristics of intensification and diversification in these algorithms. The effectiveness or ineffectiveness of a meta-heuristic algorithm obviously relies upon a proper trade-off between exploration and exploitation. If the trade-off is poor, then it will result in an unacceptable optimization approach. Amongst meta-heuristic algorithms, the PSO algorithm and its variants are used popularly in the optimal operation problem, because they are simpler to implement than other existing optimization algorithms [8]. However, the PSO algorithms are easy to be stuck in a local optimum and result in premature convergence [23]. Recently, the CS algorithm is also applied to resolve the optimal operation problem however, its convergence capability is sometimes poor [9].

This paper proposes a MCS algorithm for the optimal operating problem of the integrated energy systems. The proposed MCS algorithm is to optimize the fuel cost, emission, and risk cost of the integrated IEEE 10-generator energy system. The paper is organized as follows. The integrated energy system including thermal, solar and wind plants and a load model is described in Section 2. The optimization of the integrated energy system is introduced in Section 3. A novel application of a MCS algorithm for the optimal operating problem is proposed in Section 4. The obtained results and comparisons follow to validate the proposal in Section 5. Finally, the proposal's advantages are summarized in Section 6.

2. Integrated energy systems

An optimization of the integrated energy system is obtained by harvesting maximum renewable energy during its availability. The integrated energy system includes the thermal, solar and wind plants in this paper, where solar power is produced either by solar PV panels, solar thermal plants, or both, while wind power is produced by wind turbines. The solar and wind powers are presented in sections 2.1-2.2 followed by a description of the load model.

2.1. Solar energy source

The power of solar PV panels is obtained at the maximum power point (MPP) as follows [8]:

$$P_{PV} = \left[P_{PV,STC} \times \frac{G_T}{1000} \times \left[1 - c_t \times \left(T_C^0 - 25 \right) \right] \right] \times N_{PVs} \times N_{PVp} \quad (1)$$

where P_{PV}: The PV power at the MPP (W), $P_{PV,STC}$: The rated PV power at the MPP and standard testing condition (STC) (W), G_T: The irradiation level (W/m^2), c_t: The power temperature coefficient at the MPP (%/^{0}C), *T:* The cell temperature (^{0}C), N_{PVs} and N_{PVp}: The number of modules in series and in parallel composing the PV generator, respectively.

The power of a solar thermal plant is given by:

$$P_{Ther} = \eta \times A_c \times G_T \quad (2)$$

where P_{Ther}: The power of a solar thermal plant (W), η: The collector efficiency, and A_c: The collector area (m^2).

2.2.Wind energy source

The mechanical power recovered by a wind turbine is given by [8]:

$$P_{wind} = \frac{1}{2} \times C_e \times \rho \times A_s \times V_{wind}^3 \quad (3)$$

where P_{wind}: The mechanical power of a wind turbine (W), C_e: The efficiency factor depending on the wind speed and the system architecture, ρ: The density of air (kg/m^3), ρ=1.225 kg/m^3, A_s: The surface area traversed by the wind (m^2), and V_{wind}: the wind speed (m/s).

2.3. Load model

It is obvious that the above integrated energy system depends on uncontrollable natural conditions forming challenges for optimizing. In order to simplify this issue, the harvested solar and wind powers are assumed as negative loads. Then, the actual load power is given by:

$$P_{load}^{Actual} = P_{load}^{Total} - \left(P_{solar} + P_{wind} \right) \quad (4)$$

where P_{load}^{Actual} : the actual load power (W), P_{load}^{Total} : the total load power (W), P_{solar} : the solar generation power (W), and P_{wind} : the wind generation power (W).

3.Optimization of integrated energy systems

In this paper, the optimization is to minimize the objective functions of the fuel cost, emission and risk cost with several equality and inequality constraints. Based on the characteristics of thermal, solar and wind power generations, this multi-objective optimal operation is established as follows.

3.1. Objective function

3.1.1. Economic benefit based objective function

The economic benefit based objective function, f_1 is based on the fuel cost curves of thermal generators which are quadratic functions with a sine component to represent the valve loading effects. It is given by [8]:

$$f_1 = C(P_G) = \sum_{i=1}^{N_g} a_i + b_i P_{Gi} + c_i P_{Gi}^2 + \left| d_i \sin\left[e_i \left(P_{Gi} - P_{Gi}^{\min} \right) \right] \right| \tag{5}$$

where $C(P_G)$: the total fuel cost \$/h, a_i, b_i and c_i: the cost coefficients of the i^{th} generator, d_i and e_i: the cost coefficients of the i^{th} generator reflecting valve-point effects, P_{Gi}: the active output power of the i^{th} generator (W), P_{Gi}^{min}: the lower limit of the active output power of the i^{th} generator (W), P_{Gi}^{max}: the upper limit of the active output power of the i^{th} generator (W), P_G: the vector of the active output powers of generators defined as follows: $P_G = [P_{G1}, P_{G2}, \ldots, P_{GNg}]$, and N_g: the total number of thermal generators in a power system.

3.1.2. . Environmental benefit based objective function

The environmental benefit based objective function, f_2 is based on the total emission of atmospheric pollutants such as sulphur oxides, SO_x and nitrogen oxides, NO_x caused by fossil-fuelled thermal power plants. It is described by the polynomial and exponential terms of thermal generators as follows [24]:

$$f_2 = E(P_G) = \sum_{i=1}^{N_g} \alpha_i + \beta_i P_{Gi} + \gamma_i P_{Gi}^2 + \xi_i \exp(\omega_i P_{Gi}) \tag{6}$$

where $E(P_G)$: the total emission (ton/h), and α_i, β_i, γ_i, ξ_i and ω_i: the emission coefficients of the i^{th} generator.

3.1.3. . Social benefit based objective function

The social benefit based objective function, f_3 is based on a risk cost caused by solar and wind powers. The risk is the power outage producing social losses. It is as follows [14]:

$$f_3 = R_t P_{load}^{Actual} \tag{7}$$

$$R_t = \begin{cases} 1 - \dfrac{P_{reserved}^t}{P_{renewable}^t}, & P_{reserved}^t < P_{renewable}^t \\ 0, & P_{reserved}^t \geq P_{renewable}^t \end{cases} \tag{8}$$

where R_t: the coefficient of the risk cost in t^{th} hour caused by solar and wind powers ($/hW), $P^t_{reserved} = P_{Gi}{}^{max} - P_{Gi}{}^t$: the spinning power reserved in t^{th} hour (W), and $P^t_{renewable}$: the output solar and wind powers in t^{th} hour (W).

3.2. Constraint conditions

The constraint conditions including power balance, power operation limit, ramp rate limit, and security operation are as follows:

3.2.1. Power balance

The power balance constraint is described by:

$$\sum_{i=1}^{N_g} P_{Gi} = P_{load}^{Actual} + P_{loss} \tag{9}$$

$$P_{loss} = \sum_{i=1}^{N_g}\sum_{j=1}^{N_g} P_{Gi} B_{ij} P_{Gj} + \sum_{i=1}^{N_g} B_{i0} P_{Gi} + B_{00} \tag{10}$$

where P_{loss}: the active power loss in transmission lines (W), and B_{ij}, B_{i0} and B_{00}: the *B*-coefficients of the power loss of the power system which depend on the impedance parameters of the transmission lines.

3.2.2. . Power operation limit

The power generation should be within the minimum and maximum limits as follows:

$$P_{Gi}^{\min} \le P_{Gi} \le P_{Gi}^{\max},\ i = 1, \ldots, N_g \tag{11}$$

$$0 \le P_{solar} \le P_{solar}^{\max} \tag{12}$$

$$0 \le P_{wind} \le P_{wind}^{\max} \tag{13}$$

where $P_{solar}^{\max}$: the upper limit of the solar generation power (W), and $P_{wind}^{\max}$: the upper limit of the wind generation power (W).

3.2.3. Ramp up and down rate power limit

The ramp up and down rate power constraints for thermal generating units are described as follows:

$$P_{G_i(t)} - P_{G_i(t-1)} \le P_{G_i}^{up} \tag{14}$$

$$P_{G_i(t-1)} - P_{G_i(t)} \le P_{G_i}^{down} \tag{15}$$

where $P_{G_i}^{up}$ and $P_{G_i}^{down}$: the ramp up and down rate power limits of the i^{th} generator, respectively (W).

3.2.4. . Security operation

For security operation, the transmission line loading, S_l is restricted by its upper limit as follows:

$$S_{li} \le S_{li}^{\max},\ i=1, \ldots, n_l \tag{16}$$

where S_{li}: the transmission line loading, S^{max}_{li}: the upper limit of the transmission line loading, and n_l: the number of transmission lines.

3.3. Optimization model

This paper presents the three optimization models for integrated energy systems including the economic optimization model; the economic and environmental optimization model; and the economic, environmental, and social optimization model. The description of each optimization model is detailed as follows:

The economic optimization model is based on the fuel cost function of thermal generators. Then, the objective function, f_1 is minimized.

The economic and environmental optimization model is described by the functions of the fuel cost and the emission respectively, f_1 and f_2. This is to optimize the fuel cost and the emission of thermal generators.

The economic, environmental, and social optimization model is established by the functions of the fuel cost, the emission, and the risk cost respectively, f_1, f_2 and f_3. This model is optimized to ensure that the fuel cost and the emission of thermal generators as well as the risk cost caused by solar and wind powers are minimal. The MCS algorithm is proposed to solve the models of the economic optimization; the economic and environmental optimization; and the economic, environmental, and social optimization of the integrated energy system with the thermal, wind and solar powers.

4. Modified cuckoo search algorithm based optimization.

The CS algorithm is a stochastic global search algorithm based on the interesting breeding behaviour such as brood parasitism of certain species of cuckoos [25]. The CS and MCS algorithms are presented in detail in sections 4.1 - 4.2.

4.1. Cuckoo search algorithm

The breeding strategy of some cuckoos by laying their eggs in the nest of host birds is utilized where the cuckoo randomly chooses the nest position to lay an egg that is a new solution, $P_{G_i,k}^{iter+1}$ in the optimization through the Lévy flight behaviour [25].

$$P_{G_i,k}^{iter+1} = P_{G_i,k}^{iter} + \varepsilon \oplus Levy(\sigma) \tag{17}$$

where $\varepsilon > 0$: the step size, k: the k^{th} host nest, k=[1,…, m], l: the l^{th} random nest, l=[1,…, m], m: the number of the host nest, *iter*: the *iter*$^{\text{th}}$ iteration, $Iter_{max}$: the number of maximum iterations, $\oplus$: the product of the entry wise multiplications, and p_a: the possibility of an alien egg to be discovered by host bird, $p_a \in [0, 1]$.

The step length, Lévy(σ) is given by:

$$\text{Lévy}(\sigma) = t^{-\sigma},\ \sigma \in (1, 3] \tag{18}$$

The flowchart of the CS algorithm applied for the optimal operating problem is shown as in Fig. 1.

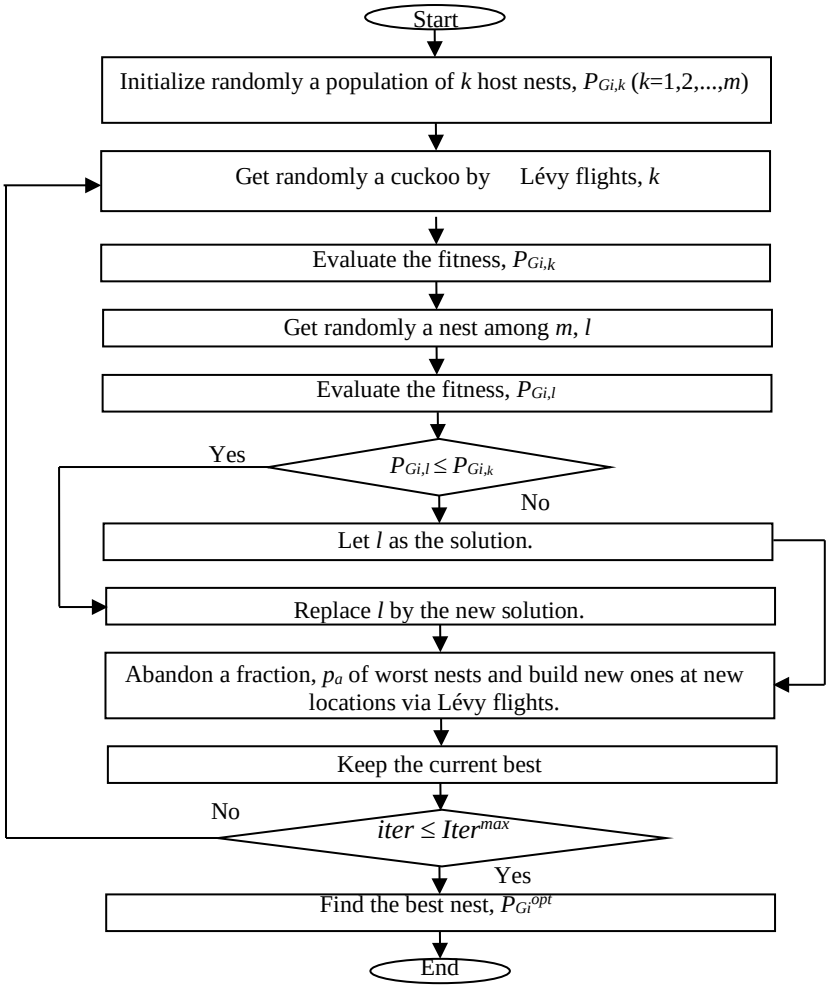

Fig. 1. CS algorithm flowchart applied for the optimal operating problem.

4.2. Modified cuckoo search algorithm

It is obvious that the CS algorithm is always converged, however the convergence speed and value are sometimes poor. A MCS algorithm has been introduced to improve the convergence for optimizing of the integrated energy system. The objective functions are in (5)-(8) as well as the equality and inequality constraints are in (9)-(16).The modifications are described as follows [26]:

The first modification is made to the Lévy flight step size, ε that is a constant value, ε=1 [25] in the CS algorithm. This affected the ability of the localized searching when the solution gets closer to the best one. In the MCS algorithm, the value of ε is made to decrease as the number of generations increases so that the searching performance is improved. An initial value of the Lévy flight step size, ε_0=1 is chosen and then, a new Lévy flight step size is calculated at each generation as follows:

$$\varepsilon_i = \frac{\varepsilon_0}{\sqrt{iter}} \tag{19}$$

where ε_0: The initial value of the Lévy flight step size.

The second modification is to speed up the convergence by adding information exchange between top solutions which is not available in the CS algorithm. The information exchange in the MCS algorithm is described as follows:

A fraction of the eggs with the best fitness are put into a group of top elite eggs and each of the top elite eggs randomly picks a second elite egg. A new egg is then generated along the line connecting these two top elite eggs. If both eggs have the same fitness, then the new egg will be generated at the midpoint. There is a possibility that the same egg is picked twice in this step. In this case, a local Lévy flight search is performed from the randomly picked nest that the Lévy flight step size, ε is given by:

$$\varepsilon_i = \frac{\varepsilon}{iter^2} \tag{20}$$

The MCS algorithm is proposed to find out optimal powers, P_{Gi} in order to ensure the optimization of the economic, environmental, and social benefits of the integrated energy system.

5. Numerical Results

The numerical results of the optimal operating problems are implemented on the integrated IEEE 10-generator energy system with the solar and wind energy sources by using the MCS algorithm is shown in Fig. 2.

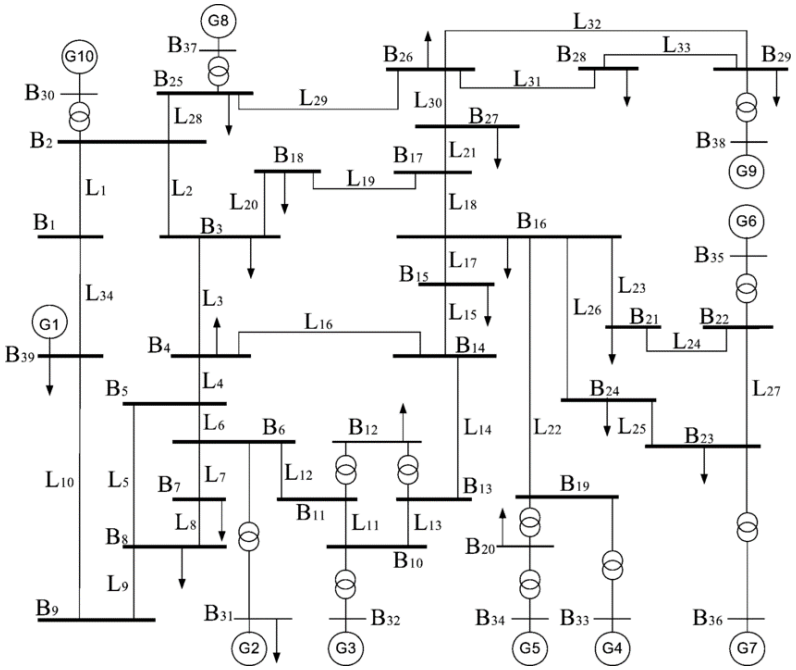

Fig. 2. IEEE 10-generator energy system.

The fuel cost coefficients and active generation limits; the emission coefficients; and the values of the *B*-coefficients matrix for the IEEE 10-generator energy system are in Tables 1-3 [25→24]. The solar power, P_{solar} including the PVs' power, P_{pv} and the power of solar thermal plants, P_{Ther} as well as the power of wind turbines, P_{wind} *of* the 24 hours are assumed; and then, the total and actual load demands are calculated as in Table 4. The upper limits of the solar and wind generation powers are 100 MW. The ramp up and down rate power limits of the i^{th} generator is set as 10% of its maximum power. Figure 3 obviously shows that the total power of traditional thermal generators has been cut down by the solar and wind powers. The average reduction is 22.64%. In the period of 8 h - 12 h, the total power of the renewable energy sources generated is highest, 170 MW including the solar power, P_{solar} = 90 MW and the wind power, P_{wind} = 80 MW. Furthermore, the percentage of the total power of traditional thermal generators cut down is largest in the period of 5 h - 8 h, 26.79%. These positively impact on the factors concerning the fuel cost and emission minimization of the power system. This also confirms a tendency towards modern power systems including renewable energy sources in the future. Table 5 shows the parameters of the CS and MCS algorithms. The difference between these two algorithms is the chosen value of the Lévy flight step size, ε.

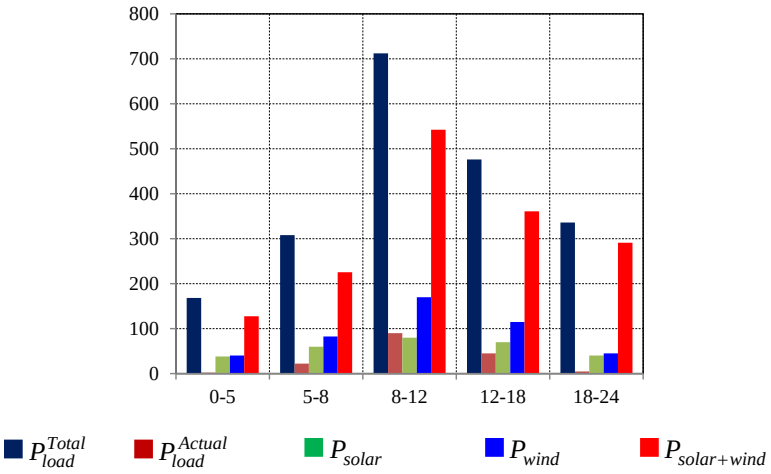

Fig. 3. Total and actual load powers and the solar and wind powers obtained.

Table 1. Fuel cost coefficients and active power generation limits of the IEEE 10-generator energy system.

G_i	a_i	b_i	c_i	d_i	e_i	P_{Gi}^{min}	P_{Gi}^{max}
1	1000.403	40.5407	0.12951	33	0.0174	10	55
2	950.606	39.5804	0.10908	25	0.0178	20	80
3	900.705	36.5104	0.12511	32	0.0162	47	120
4	800.705	39.5104	0.12111	30	0.0168	20	130
5	756.799	38.5390	0.15247	30	0.0148	50	160
6	451.325	46.1592	0.10587	20	0.0163	70	240
7	1243.531	38.3055	0.03546	20	0.0152	60	300
8	1049.998	40.3965	0.02803	30	0.0128	70	340
9	1658.569	36.3278	0.02111	60	0.0136	135	470
10	1356.659	38.2704	0.01799	40	0.0141	150	470

Table 2. Emission coefficients of the IEEE 10-generator energy system.

G_i	α_i	β_i	γ_i	ξ_i	ω_i
1	360.0012	-3.9864	0.04702	0.25475	0.01234
2	350.0056	-3.9524	0.04652	0.25475	0.01234
3	330.0056	-3.9023	0.04652	0.25163	0.01215
4	330.0056	-3.9023	0.04652	0.25163	0.01215
5	13.8593	0.3277	0.00420	0.24970	0.01200
6	13.8593	0.3277	0.00420	0.24970	0.01200
7	40.2669	-0.5455	0.00680	0.24800	0.01290
8	40.2669	-0.5455	0.00680	0.24990	0.01203
9	42.8955	-0.5112	0.00460	0.25470	0.01234
10	42.8955	-0.5112	0.00460	0.25470	0.01234

Table 3. Values of the B-coefficient matrix for the IEEE 10-generator energy system.

$$[B]=10^{-6}\times\begin{bmatrix} 49 & 14 & 15 & 15 & 16 & 17 & 17 & 18 & 19 & 20 \\ 14 & 45 & 16 & 16 & 17 & 15 & 15 & 16 & 18 & 18 \\ 15 & 16 & 39 & 10 & 12 & 12 & 14 & 14 & 16 & 16 \\ 15 & 16 & 10 & 40 & 14 & 10 & 11 & 12 & 14 & 15 \\ 16 & 17 & 12 & 14 & 35 & 11 & 13 & 13 & 15 & 16 \\ 17 & 15 & 12 & 10 & 11 & 36 & 12 & 12 & 14 & 15 \\ 17 & 15 & 14 & 11 & 13 & 12 & 38 & 16 & 16 & 18 \\ 18 & 16 & 14 & 12 & 13 & 12 & 16 & 40 & 15 & 16 \\ 19 & 18 & 16 & 14 & 15 & 14 & 16 & 15 & 42 & 19 \\ 20 & 18 & 16 & 15 & 16 & 15 & 18 & 16 & 19 & 44 \end{bmatrix}$$

Table 4. Total and actual load demands of 24 hours.

t (h)	P_{load}^{Total} (MW)	P_{solar} (MW)	P_{wind} (MW)	$P_{solar}+P_{wind}$ (MW)	P_{load}^{Actual} (MW)	$\Delta\sum P_{Gi}$ (%)
0-5	168.00	2.25	38.00	40.25	127.75	23.96
5-8	308.00	22.50	60.00	82.50	225.50	26.79
8-12	712.00	90.00	80.00	170.00	542.00	23.88
12-18	476.00	45.00	70.00	115.00	361.00	24.16
18-24	336.00	5.00	40.00	45.00	291.00	13.39
Total	2000.00	164.75	288.00	452.75	1547.25	22.64

Table 5. Parameters of the CS and MCS algorithms.

Parameter	Value	
	CS	MCS
Number of nests, m	10	10
Number of maximum iterations, $Iter^{max}$	200	200
Lévy flight step size, ε	0.5	Using (18) and (19)
Possibility of alien egg, p_a	0.6	0.6

In the numerical results, the Lévy flight step size is a constant value, ε=0.5 in the CS algorithm and is a generation-varying variable in the MCS algorithm. This is to improve the convergence ability of the CS algorithm including the convergence speed and value. In both the CS and MCS algorithms, the number of nests is 10; the number of maximum iterations is 200; and the probability of an alien egg is 0.6. Figures 4-8 show the convergence characteristics of the fuel cost minimization with the solar and wind energy sources using the CS and MCS algorithms. With the CS algorithm, the

economic optimization problem converges at the 39th, 44th, 43rd, 41st and 40th iterations whereas with the MCS algorithm, it converges at the 14th, 15th, 16th, 17th, and 16th iterations in the periods of 0 h - 5 h, 5 h - 8 h, 8 h - 12 h, 12 h - 18 h and 18 h - 24 h respectively. It is obvious that the convergence speed of the MCS algorithm is always faster than that of the CS algorithm.

Furthermore, in the period of 0 h - 5 h, the optimal fuel costs are 0.0559×10^5 \$/h, 0.0598×10^5 \$/h, 0.0617×10^5 \$/h and 0.0643×10^5 \$/h using the MCS, CS, Chaos PSO and time varying acceleration based PSO (TVAC-PSO) algorithms respectively which show that the convergence value of the MCS algorithm is better than that of the CS, Chaos PSO and TVAC-PSO algorithms in the economic optimization, Table 6. This is also similar in the periods of 5 h - 8 h, 8 h - 12 h, 12 h - 18 h and 18 h - 24 h. Obviously, both the convergence speed and value are improved using the MCS algorithm compared with the CS, Chaos PSO and TVAC-PSO algorithms in the economic optimization. The improvement is due to the Lévy flight step size being made to decrease as the number of generations increases in order to improve the searching performance as well as there is the information exchange between the solutions in an attempt to speed up convergence to an optimal solution.

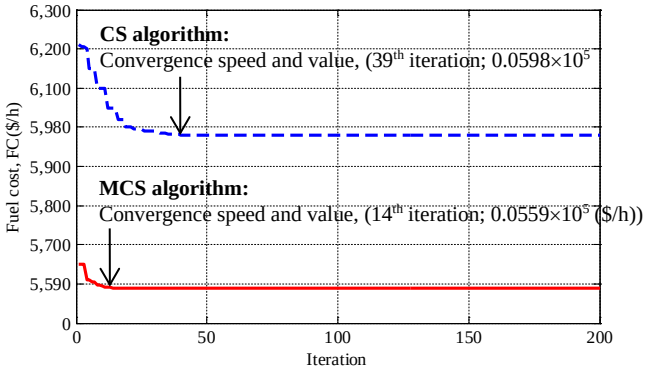

Fig. 4. Convergence characteristic of the fuel cost minimization with the solar and wind energy sources using the CS and MCS algorithms, t=(0-5)h.

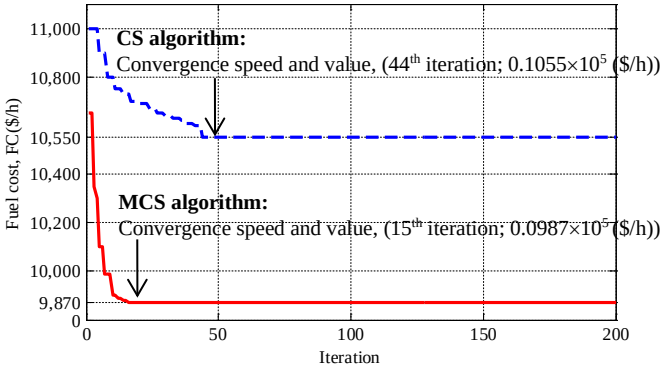

Fig. 5. Convergence characteristic of the fuel cost minimization with the solar and wind energy sources using the CS and MCS algorithms, t=(5-8)h.

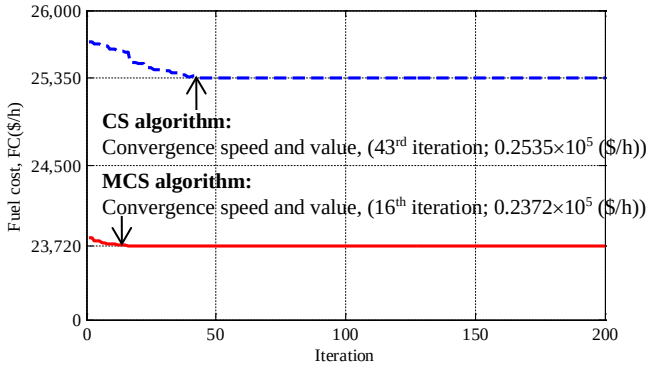

Fig. 6. Convergence characteristic of the fuel cost minimization with the solar and wind powers using the CS and MCS algorithms, t=(8-12)h.

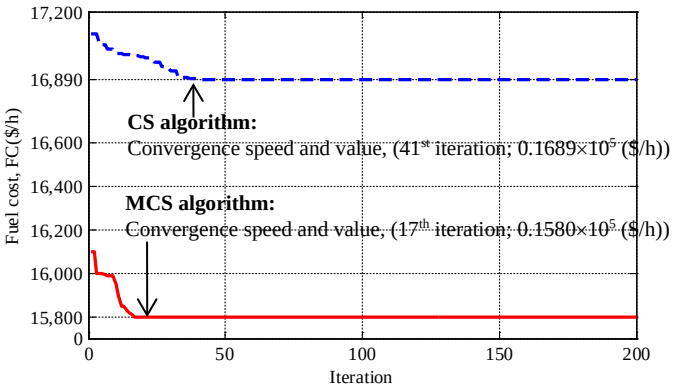

Fig. 7. Convergence characteristic of the fuel cost minimization with the solar and wind powers using the CS and MCS algorithms, t=(12-18)h.

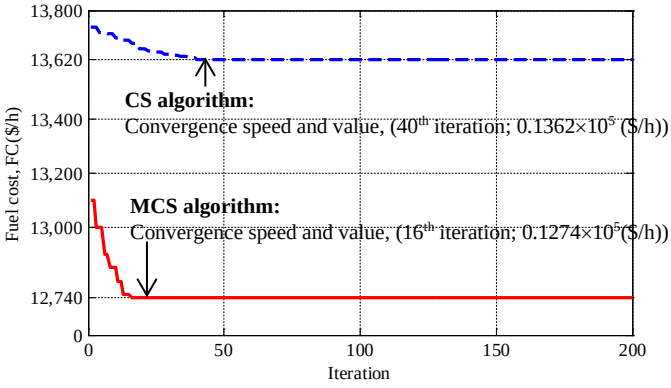

Fig. 8. Convergence characteristic of the fuel cost minimization with the solar and wind powers using the CS and MCS algorithms, t=(18-24)h.

Tables 6-8 show the best solutions for the economic optimization problem of the fuel cost minimization; the economic and environmental optimization problem of the fuel cost and emission minimization; and the economic, environmental, and social optimization problem of the total cost and emission minimization of the integrated IEEE 10-generator energy system using the MCS, CS, Chaos PSO and TVAC-PSO algorithms. In the period of 0 h - 5 h, using the MCS algorithm, the optimal total cost is 0.0559×10^5 \$/h in the economic optimization problem, Table 6. The optimal total cost is 0.0440×10^5 \$/h in the economic and environmental problem, Table 7 which is significantly reduced as compared with the optimal total cost, 0.0559×10^5 \$/h in the economic optimization problem, Table 6.

The reduction percentage of the total cost is 21.29%. Additionally, the optimal total cost is 0.0463×10^5 \$/h in the economic, environmental, and social optimization problem, Table 8 which is a little higher than the optimal total cost, 0.0440×10^5 \$/h in the economic and environmental optimization problem, Table 7. The increment percentage is 4.97%. This is due to the consideration of the social benefit in the economic, environmental, and social optimization problem. Then, the total cost in the economic, environmental, and social optimization problem is increased compared with this in the economic and environmental problem. Obviously, it is necessary to consider the social benefit to manage the risk of power systems integrated with the solar and wind energy sources because of their randomness.

The result analysis is the same in the periods of 5 h - 8 h, 8 h - 12 h, 12 h - 18 h and 18 h - 24 h which shows the MCS algorithm's stability in both the convergence speed and value. Similarly, in the period of 0 h - 5 h, the optimal emission amounts are 233.4862 (ton/h); 254.2705 (ton/h); 257.5096 (ton/h) and 269.9262 (ton/h) using the MCS, CS, Chaos PSO and TVAC-PSO algorithms, respectively. This also shows that the convergence value of the MCS algorithm is better than that of the CS, Chaos PSO and TVAC-PSO algorithms in the economic and environmental optimization. This is also the same in the periods of 5 h - 8 h, 8 h - 12 h, 12 h - 18 h and 18 h - 24 h, Table 7. The MCS algorithm also shows its advantages in the convergence values of the optimal total cost and emission amount of the economic, environmental, and social optimization in the periods of 0 h - 5 h, 5 h - 8 h, 8 h - 12 h, 12 h - 18 h and 18 h - 24 h, Table 8.

Table 9 shows the comparison of the best solution for the economic, environmental, and social optimization of the total cost and emission minimization of the IEEE 10-generator energy system with and without the solar and wind powers using the MCS algorithm. In the period of 0 h - 5 h, the total costs are 0.0463×10^5 \$/h and 0.0538×10^5 \$/h respectively with and without the solar and wind powers. The total cost reduction is 0.0075×10^5 \$/h and the improvement percentage of the total cost is 13.96%.

Table 6. Comparison of the best solution for the optimal economic operation of the fuel cost minimization with the solar and wind energy sources using TVAC-PSO and Chaos PSO, CS and MCS algorithms.

t (h)	Fuel cost, FC \$/h×10^5			
	TVAC-PSO	Chaos PSO	CS	MCS
0-5	0.0643	0.0617	0.0598	0.0559
5-8	0.1134	0.1089	0.1055	0.0987
8-12	0.2726	0.2617	0.2535	0.2372
12-18	0.1816	0.1743	0.1689	0.1580
18-24	0.1464	0.1405	0.1362	0.1274

Table 7. Comparison of the best solution for the optimal economic and environmental operation of the fuel cost and emission minimization with the solar and wind energy sources using TVAC-PSO and Chaos PSO, CS and MCS algorithms.

t (h)	TVAC-PSO		Chaos PSO		CS		MCS	
	Fuel cost, FC $/h× 10^5	Emission, E (ton/h)	Fuel cost, FC $/h× 10^5	Emission, E (ton/h)	Fuel cost, FC $/h× 10^5	Emission, E (ton/h)	Fuel cost, FC $/h× 10^5	Emission, E (ton/h)
0-5	0.0508	269.9262	0.0486	257.5096	0.0478	254.2705	0.0440	233.4862
5-8	0.0896	476.4646	0.0857	454.5472	0.0842	448.8297	0.0777	412.1419
8-12	0.2154	1145.2054	0.2061	1092.5260	0.2025	1078.7835	0.1868	990.6027
12-18	0.1435	762.7659	0.1373	727.6787	0.1349	718.5255	0.1244	659.7925
18-24	0.1157	614.8612	0.1107	586.5776	0.1088	579.1993	0.1003	531.8549

Table 8. Comparison of the best solution for the optimal economic, environmental, and social operation of the total cost and emission minimization with the solar and wind energy sources using TVAC-PSO, Chaos PSO, CS and MCS algorithms.

t (h)	TVAC-PSO		Chaos PSO		CS		MCS	
	Total cost, TC $/h×$10^5$	Emission, E(ton/h)	Total cost, TC $/h×$10^5$	Emission E (ton/h)	Total cost, TC $/h×$10^5$	Emission , E (ton/h)	Total cost, TC $/h× 10^5	Emission, E (ton/h)
0-5	0.0558	262.6382	0.0531	247.7242	0.0519	243.8454	0.0463	215.0408
5-8	0.0983	463.6001	0.0937	437.2744	0.0916	430.4276	0.0817	379.5827
8-12	0.2364	1114.2849	0.2253	1051.0100	0.2201	1034.5534	0.1965	912.3451
12-18	0.1575	742.1712	0.1501	700.0269	0.1466	689.0659	0.1309	607.6689
18-24	0.1270	598.2599	0.1210	564.2876	0.1182	555.4521	0.1055	489.8384

Table 9. Comparison of the best solution for the optimal economic, environmental, and social operation of the total cost and emission minimization with and without the solar and wind powers using MCS algorithm.

t (h)	Without the solar and wind powers		With the solar and wind powers		Comparison between with and without the solar and wind powers			
	Total cost, TC $/h×$10^5$	Emission, E(ton/h)	Total cost, TC $/h×$10^5$	Emission, E(ton/h)	ΔTC $/h×$10^5$	ΔTC (%)	ΔE (ton/h)	ΔE (%)
0-5	0.0538	226.7605	0.0463	215.0408	0.0075	13.96	11.7197	5.17
5-8	0.0960	418.1483	0.0817	379.5827	0.0143	14.92	38.5656	9.22
8-12	0.2277	1060.4187	0.1965	912.3451	0.0312	13.70	148.0736	13.96
12-18	0.1524	688.7319	0.1309	607.6689	0.0215	14.13	81.0630	11.77
18-24	0.1160	527.3110	0.1055	489.8384	0.0105	9.07	37.4726	7.11
TOTAL	0.6460	2921.3705	0.5609	2604.4759	0.0851	13.17	316.8946	10.85

Similarly, the emission amounts are 215.0408 (ton/h) and 226.7605 (ton/h) respectively with and without the solar and wind powers. The emission reduction is 11.7197 (ton/h) and the improvement percentage of the emission amount is 5.17%. Obviously, the improved percentages of the total cost and the emission amount are always higher than 9% and 5% respectively by integrating the solar and wind powers. Especially, the improved percentage of the total cost is highest in the period of 5 h -

8 h with 14.92%, since the percentage of the total power of traditional thermal generators cut down is largest in the period of 5 h - 8 h, 26.79%.

The improved percentage of the emission amount is highest in the period of 8 h - 12 h with 13.96%. This is due to the solar and wind powers generated are highest, 170 MW in the period of 8 h - 12 h. These show the effectiveness of integrating solar and wind powers into the energy system in the total cost and emission amount. However, it is obvious that this research also has several issues which need to be detailed in the future work such as the consideration of the cost functions of the solar and wind power sources, as well as the effect of the real time weather condition in the optimal operation.

6. Conclusions

The paper proposed the optimization model of the integrated energy system detailed in the optimization of the economic, environmental, and social benefits. Especially, the optimization of the social benefit which is based on the risk cost of the solar and wind power sources, has been mentioned in this paper. This contribution is valuable and necessary as the solar and wind power systems are increasingly encouraged to integrate into the traditional power system of the thermal and hydro power sources. In order to solve this multi-objective optimal operation problem, the MCS algorithm is a variant of the CS algorithm with the generation varying Lévy flight step size which has been proposed to find out an optimal solution for the integrated energy system.

The obtained numerical results indicated that the fuel cost, emission, and risk cost of the integrated energy system are always less than those without the integration. It means that the solar and wind powers have efficiently supported to optimize the economic, environmental, and social benefits.

Furthermore, the achieved results also validated the proposed application of the MCS algorithm for the optimal operation. It is obvious that the results of using the MCS algorithm are always better than those of using the CS, Chaos PSO and TVAC-PSO algorithms in the convergence speed and value. These results are particularly important in the optimal operation of the power system taking into account the renewable energy sources.

References

1. Lee, S.; and Shim, H. (2019). Distributed algorithm for economic dispatch problem with separable losses. *IEEE Control Systems Letters*, 3(3), 685-690.
2. Sulaiman, M.H.; Mustaffa, Z.; and Aliman, O. (2019). An application of barnacles mating optimizer for solving economic dispatch problems. *Proceeding of the first IEEE Jordan International Joint Conference on Electrical Engineering and Information Technology*. Amman, Jordan, 112-117.
3. Chansareewittaya, S. (2018). Hybrid BA/ATS for economic dispatch problem. *Proceeding of the 22nd International Computer Science and Engineering Conference*. Chiang Mai, Thailand, 568-573.
4. Mei, J.; and Zhao, J. (2018). An enhanced quantum-behaved particle swarm optimization for security constrained economic dispatch. *Proceeding of the 17th International Symposium on Distributed Computing and Applications for Business Engineering and Science.* Wuxi, China, 921-926.

5. Valluuru, H.V.; Khandavilli, S.; Sela, N.V.S.K.C.; Thota, P.R.; and Muktevi, L.N.V. (2018). Modified TLBO technique for economic dispatch problem. *Proceeding of the Second International Conference on Intelligent Computing and Control Systems.* Madurai, India, 1970-1973.
6. Mohamed, F.; Abdel-Nasser, M.; Mahmoud, K.; and Kamel, S. (2018). Economic dispatch using stochastic whale optimization algorithm. *Proceeding of the First International Conference on Innovative Trends in Computer Engineering.* Aswan, Egypt, 19-24.
7. Absil, P.A.; Sluysmans, B.; and Stevens, N. (2018). MIQP-based algorithm for the global solution of economic dispatch problems with valve-point effects. *Proceeding of the First Power Systems Computation Conference.* Dublin, Ireland, 56-62.
8. Huynh, D.C.; and Nirmal, N. (2015). Chaos PSO algorithm based economic dispatch of hybrid power systems including solar and wind energy sources. *Proceeding of the First IEEE Innovative Smart Grid Technologies-Asia.* Bangkok, Thailand, 1-6.
9. Huynh, D.C.; and Nirmal, N. (2015). Economic dispatch integrating wind power generation farms using cuckoo search algorithm. *Proceeding of the First IEEE Innovative Smart Grid Technologies-Asia.* Bangkok, Thailand, 6-12.
10. Ma, S.; Wang, Y.; and Lv, Y. (2018). Multiple environment/economic power dispatch using evolutionary multi-objective optimization. *IEEE Access*, 6(1), 13066-13074.
11. Khalil, M.; Wibowo, R.S.; and Penangsang, O. (2018). Combined economic emission dispatch with cubic criterion function using cuckoo search algorithm. *Proceeding of the First International Conference on Information and Communications Technology*, Yogyakarta, Indonesia, 36-40.
12. Liang, H.; Liu, Y.; Shen, Y.; and Li, F. (2017). A multi-objective chaotic bat algorithm for economic and emission dispatch. *Chinese Automation Congress, CAC 2017*, 1-6.
13. Lin, Z.Y.; Chiang, T.C.; and Lee, C.Y. (2017). Adaptive multiobjective differential evolution algorithms for environmental/economic dispatch. *Proceeding of 6th IIAI International Congress on Advanced Applied Informatics.* Hamamatsu, Japan, 909-914.
14. Niu, D.; and Wei, Y. (2013). A novel social-environmental-economic dispatch model for thermal/wind power generation and application. *International Journal of Innovative Computing, Information and Control*, 9(7), 3005-3014.
15. Niu, Q.; Wang, H.; and Zhang, Y. (2019). Restart covariance matrix adaptation evolution strategy for solving wind-integrated emission economic dispatch problems. *Proceeding of the First IEEE Congress on Evolutionary Computation.* Wellington, New Zealand, 1-6.
16. Tang, C.; Liang, C.; and Hu, Y. (2018). A reliable quadratic programming algorithm for convex economic dispatch with renewable power uncertainty. *Proceeding of 8th International Conference on Power and Energy Systems*, Colombo, Sri Lanka, 40-43.
17. Sadoudi, S.; Boudour, M.; and Kouba, N.E.Y. (2018). Optimal combined dynamic economic and emission dispatch including wind and photovoltaic

power systems. *Proceeding of the First International Conference on Electrical Sciences and Technologies in Maghreb*. Algiers, Algeria,1-6.

18. Liu, G.; Zhu, Y.L.; and Jiang, W. (2018). Wind-thermal dynamic economic emission dispatch with a hybrid multi-objective algorithm based on wind speed statistical analysis. *IET Generation, Transmission and Distribution*, 12(17), 3972-3984.
19. Qingqing, Y.; Zhenshu, W.; Tiantian, S.; Wenqiao, L.; and Fayu, C. (2019). Environmental and economic dispatch with photovoltaic and wind power. *Proceeding of the First IEEE Sustainable Power and Energy Conference.* Beijing, China, 1-6.
20. Abu-Elzait, S.; and Parkin, R. (2019). Economic and environmental advantages of renewable-based microgrids over conventional microgrids. *Proceeding of the First IEEE Green Technologies Conference.* Los Angeles, USA, 1-6.
21. Chowdhury, F.F.; Ndoye, M.; and Murphy, G.V. (2019). Distributed combined emission-economic dispatch via coalitional integration of wind turbines. *Proceeding of the First SoutheastCon.* Alabama, USA, 1-6.
22. Spea, S.R. (2019). Combined economic emission dispatch solution of an isolated renewable integrated micro-grid using crow search algorithm. *Proceeding of the 21th International Middle East Power Systems Conference,* .Cairo, Egypt, 1-6.
23. Huynh, D.C.; and Dunnigan, M.W. (2010). Parameter estimation of an induction machine using advanced particle swarm optimization algorithms. *IET Electric Power Applications*, 4(9), 748-760.
24. Hadji, B.; Mahdad, B.; Srairi, K.; and Mancer, N. (2015). Multi-objective PSO-TVAC for environmental/economic dispatch problem. *Energy Proceedia*, 74(1), 102-111.
25. Yang, X.S.; and Deb, S. (2009). Cuckoo search via Lévy flights. *Proceeding of the First World Congress on Nature and Biologically Inspired Computing.* Coimbatore, India, 210-214.
26. Walton, S.; Hassan, O.; Morgan, K.; and Brown, M.R. (2011). Modified cuckoo search: A new gradient free optimisation algorithm. *Chaos, Solitons and Fractals*, 44(9), 710-718.